JOC The Journal of Organic Chemistry

pubs.acs.org/joc Article

Mechanistic Analysis of 5-Hydroxy γ-Pyrones as Michael Acceptor Prodrugs

Clifford Leung, Umyeena M. Bashir, William L. Karney, Mark G. Swanson, and Herman Nikolayevskiy*

Cite This: J. Org. Chem. 2024, 89, 12432−12438 Read Online

ACCESS | Metrics & More | Article Recommendations | Supporting Information

ABSTRACT: Substituted 5-hydroxy γ-pyrones have shown promise as covalent inhibitor leads against cysteine proteases and transcription factors, but their hydrolytic instability has hindered optimization efforts. Previous mechanistic proposals have suggested that these molecules function as Michael acceptor prodrugs, releasing a leaving group to generate an *o*-quinone methide-like structure. Addition to this electrophile of either water or an active site cysteine was purported to lead to inhibitor hydrolysis or enzyme inhibition, respectively. Through the use of kinetic nuclear magnetic resonance experiments, Hammett analysis, kinetic isotope effect studies, and density functional theory calculations, our findings suggest that enzyme inhibition and hydrolysis proceed by distinct pathways and are differentially influenced by substituent electronics. This mechanistic revision helps enable a more rational optimization for this class of promising compounds.

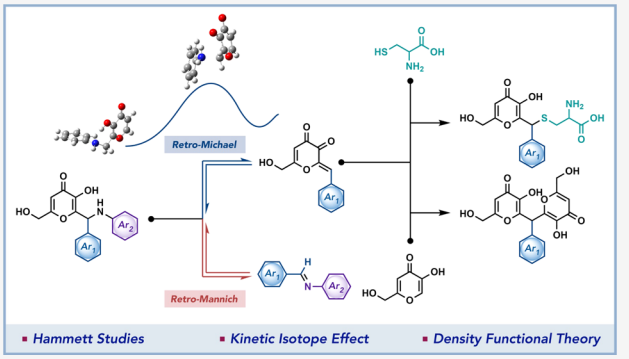

Downloaded via UNIV OF SAN FRANCISCO on September 26, 2024 at 22:25:10 (UTC).
See https://pubs.acs.org/sharingguidelines for options on how to legitimately share published articles.

INTRODUCTION

γ-Pyrones constitute a privileged class of heterocycles exhibiting a promising spectrum of pharmacological profiles ranging from antibacterial to anticancer activity.[1] Bioactive natural products containing this heterocyclic core, such as candelalide A,[2] SNF4435C(D),[3] and verticipyrone,[4] have attracted the attention of the synthetic community, leading to several published total syntheses.[5−7]

Derivatives of kojic acid, a naturally occurring 5-hydroxy γ-pyrone, have shown promise as covalent inhibitors against a variety of active site cysteines, yet their reported instability under aqueous conditions complicates structure−activity relationship (SAR) analysis and serves as a pharmacokinetic hurdle for clinical development (Figure 1).[8,9] The Williams group reported the use of **1** and two related compounds as covalent inhibitors of Cys468 against the anticancer target Stat3.[10] Although the initial results suggested a reasonable potency (IC_{50} = 10−50 μM), further development of these analogues was abandoned due to a reported loss of activity upon storage in an aqueous solution. Thereafter, the Waldmann group explored the use of **2** and its derivatives as inhibitors of Cys367 within the central pocket of TEAD (apparent IC_{50} = 8.7 μM), a transcription factor family involved in tumorigenesis.[11] Notably, Waldmann et al. reported that compounds such as **2** were stable in MES buffer (pH 6.5) but underwent noticeable degradation in HEPES buffer (pH 6.5) after 1 h. Lastly, the Jaudzems group reported **3** as a promising sortase A inhibitor targeting bacterial pathogenicity (k_{inact}/K_I = 0.0004−0.0019 μM^{-1} min^{-1}) yet also observed a loss of activity upon prolonged aqueous storage.[12] A thorough mechanistic understanding of this instability, and its relationship to the mechanism of covalent inhibition, would be critical for future rational optimization campaigns but are currently lacking.

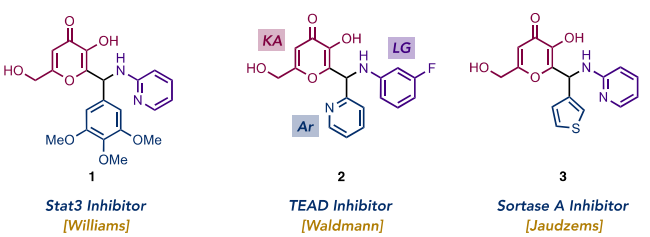

Figure 1. Kojic acid (KA) derivatives containing an aromatic ring (Ar) and an aniline leaving group (LG) serve as covalent inhibitors of active site cysteines.

5-Hydroxy γ-pyrone derivatives containing a 2-amino-pyridine or substituted aniline at the *o*-benzylic position are structurally related to aryl(β-amino)ethyl ketones,[13,14] a known class of Michael acceptor prodrugs, as well as *ortho*-substituted self-immolative linkers,[15,16] which are characterized by OH- or

Received: May 31, 2024
Revised: July 18, 2024
Accepted: August 6, 2024
Published: August 23, 2024

© 2024 American Chemical Society

https://doi.org/10.1021/acs.joc.4c01377
J. Org. Chem. 2024, 89, 12432−12438

NH-mediated 1,4-elimination of a leaving group, generating a reactive *o*-quinone methide. Similarly, kojic acid, which contains the requisite enol functionality in its hydroxy γ-pyrone core, is ideally positioned to drive the elimination of a benzylic leaving group [LG = NH-Ar_2 (Scheme 1)].

Scheme 1. Previously Proposed Mechanism for Hydrolysis and Inhibition

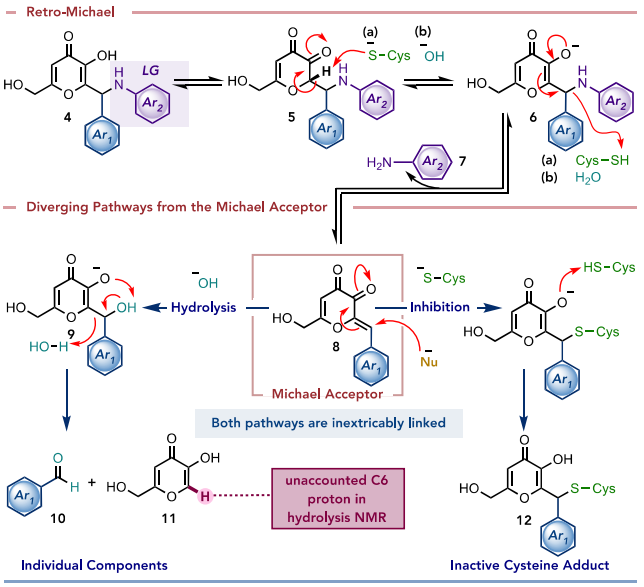

A detailed mechanism of action for this class of compounds was proposed by the Jaudzems group (Scheme 1).[12] In analogy to the mechanism of activation for aryl(β-amino)ethyl ketone inhibitors, 5-hydroxy γ-pyrone prodrug **4** was proposed to undergo tautomerization of the embedded enol to furnish dearomatized ketone **5**. Deprotonation of the reactive α-proton by an active site cysteine residue would produce enolate **6**. Notably, kojic acid derivatives are relatively acidic (pK_a = 7.9)[17] and can also be deprotonated by water at physiological pH to directly access enolate **6** from **4**. Resulting enolate **6** would mediate the β-elimination of the aniline leaving group to access *o*-quinone methide-like Michael acceptor **8**. A key cysteine residue within the enzyme's active site or transcription factor's binding interface would undergo a conjugate addition, affording inactivated cysteine adduct **12**. Hydrolytic degradation would proceed by an analogous pathway, in which a hydroxide ion adds to Michael acceptor **8** to afford hydroxy intermediate **9**. Subsequent proton transfer from the alcohol to the phenol would mediate the aldehyde scission from the kojic acid core. Degradation of hydroxy intermediate **9** could have alternatively proceeded through a retro-aldol mechanism. As the inhibition and hydrolysis pathways were proposed to proceed through the same Michael acceptor intermediate (**8**) and leaving group loss for related *o*-quinone methide prodrugs is rate-determining,[18] the two pathways are likely to share a rate-determining step. Importantly, this would signify that inhibitor reactivity and stability are inextricably linked.

The Jaudzems group conducted thorough nuclear magnetic resonance (NMR) experiments to probe their proposed mechanism, characterizing both cysteine adduct **12** and hydrolysis products **7** (LG = 2-aminopyridine), **10** (Ar_1 = thiophene), and **11**. Notably, the Jaudzems group never detected or isolated hydroxy intermediate **9**. Moreover, a close inspection of the NMR data for kojic acid byproduct **11** suggests a missing signal for the C6 position, raising the possibility of unaccounted for reactivity. In the course of our own SAR studies, inconsistencies observed with regard to the predicted versus actual stability and reactivity of 5-hydroxy γ-pyrone analogues led us to pursue a detailed mechanistic analysis of this class of compounds. Through a combination of Hammett analysis, kinetic isotope effect (KIE) studies, and density functional theory (DFT) calculations, our study elucidates the effect of substituent electronics on reaction rate and suggests that thiol addition and hydrolysis proceed by mechanistically distinct pathways.[19] This new mechanistic insight may enable strategic modifications to separately optimize the inhibitory potency and aqueous stability of this promising class of compounds.

RESULTS AND DISCUSSION

Our mechanistic study began with the synthesis of a series of *para*-substituted leaving group (LG) analogues [**L1** (Scheme 2A)]. Kojic acid, 3-nitrobenzaldehyde,[20] and an electronically

Scheme 2. General Synthesis of Analogue Libraries

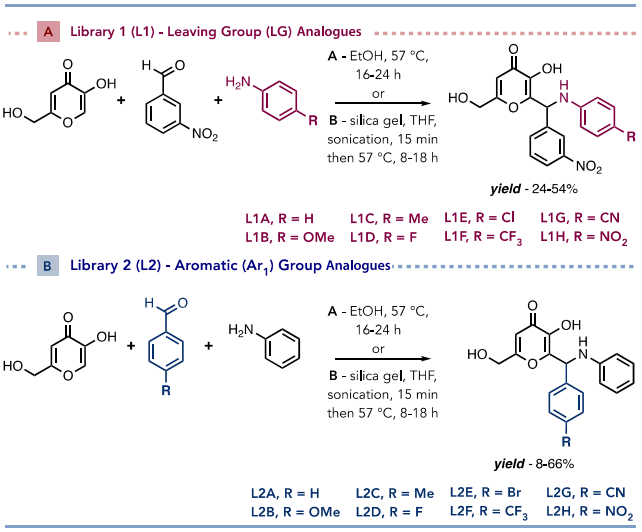

diverse set of *para*-substituted anilines were heated under standard one-pot Mannich conditions [ethanol, 16−24 h (condition A)] to selectively install the desired β-amino, β-aryl functionality at the C6 position of kojic acid.[21,22] Shorter reaction times could be achieved if the imine was preformed via sonication of a suspension of silica gel, aniline, and benzaldehyde derivatives in tetrahydrofuran for 15 min, followed by the addition of kojic acid [8−18 h (condition B)].[23] Poor to modest reaction yields (24−54%) were obtained for both electron-donating (EDGs) and electron-withdrawing groups (EWGs), largely due to hydrolytic degradation encountered under chromatographic conditions. A second library of compounds containing a range of *para*-substituted β-aryl groups (from *para*-substituted benzaldehydes) and aniline as the LG was also synthesized under similar conditions [**L2** (Scheme 2B)].

Once synthesized, each compound in the **L1** and **L2** series was subjected to an NMR kinetics assay designed to probe the rate of inhibitor consumption in the presence or absence of

https://doi.org/10.1021/acs.joc.4c01377
J. Org. Chem. 2024, 89, 12432−12438

cysteine, leading to thiol addition or hydrolysis products, respectively. To perform the NMR assays, a sample of each analogue was dissolved in $(CD_3)_2SO$ followed by the addition of an aqueous buffer solution containing dimethylmalonic acid as a quantitative internal standard. The final assay buffer contained $(CD_3)_2SO$, 1× PBS buffer, and D_2O in a 3.5:1.7:1 ratio and was adjusted to pD 7.25 (pH 6.85).[24] Notably, the use of a large amount of $(CD_3)_2SO$ in this assay was required to compensate for the poor solubility of cyano- and nitro-based analogues **L1G**, **L1H**, **L2G**, and **L2H**. For thiol addition experiments, a molar equivalent of DL-cysteine was introduced. The sample was then analyzed by NMR using water suppression with presaturation every 10 min for 3−12 h. The rate of inhibitor consumption was observed to follow first-order kinetics under all experimental conditions, and the rate constants thus obtained were analyzed using a Hammett plot [$\log(k/k_0)$ vs σ_{para}[25]].

Cysteine Experiment. In the presence of cysteine, the **L1** and **L2** series generated the expected cysteine adducts,[26] but with Hammett proportionality constants (ρ) that were inconsistent with the formation of negative charge (or loss of positive charge) on the LG nitrogen, as was initially expected from a traditional β-elimination mechanism[27] (Figure 2A). For

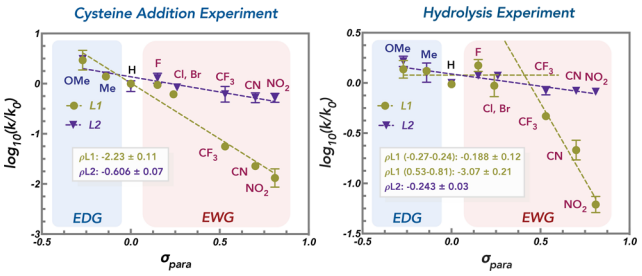

Figure 2. Hammett plots for the reactions of leaving group analogues (**L1**, yellow circle) and aryl group derivatives (**L2**, purple triangle) in the (A) presence or (B) absence of cysteine, leading to thiol addition and hydrolysis products, respectively. Reactions were conducted in triplicate at 25 °C using an assay buffer containing $(CD_3)_2SO$, 1× PBS buffer, and D_2O in a 3.5:1.7:1 ratio, adjusted to pD 7.25 (pH 6.85), with dimethylmalonic acid as an internal standard.

the **L1** series, the rate of inhibitor consumption of EDGs was significantly faster than that of EWGs, resulting in a strongly negative proportionality constant (ρ = −2.33); this would be indicative of positive charge generation on the LG nitrogen, which would be most stabilized by resonance from *para*-substituted EDGs. The **L2** series also had a negative albeit shallower slope (ρ = −0.61), suggesting that the electronics of the distal Ar_1 group played a more insignificant role in transition state stability. To explain these results, an asynchronous concerted transition state was envisioned, during which an intramolecular proton transfer between the aniline nitrogen and phenolic OH would precede and facilitate the key retro-Michael C−N scission event (Figure 3A).

DFT calculations support the mechanistic hypothesis outlined above. ω-B97X-D/6-31+G(d,p) and M06-2X/6-31+G(d,p) calculations[28,29] with PCM solvation (water)[30] were performed on model system **14**, lacking the hydroxymethyl group and the *m*-nitrophenyl group (Figure 3B).[31] The ω-B97X-D and M06-2X methods have both been shown to perform well for energetics (including barrier heights) of organic reactions.[28,29] Additional validation was achieved by

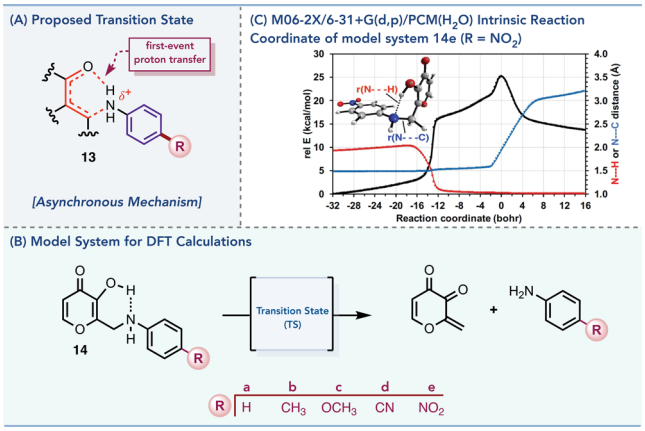

Figure 3. (A) Transition state **13** of a proposed asynchronous concerted mechanism, during which an initial intramolecular proton transfer generates δ^+ on the leaving group nitrogen. (B) Model system **14** used in computational studies with optimized geometries. (C) M06-2X/6-31+G(d,p)/PCM(H_2O) intrinsic reaction coordinate for model system **14e** (R = NO_2). Black for the relative energy, red for the N···H distance (angstroms), and blue for the N···C distance (angstroms). The structure shown is that of the reactant, corresponding to a point at the far left of the plot.

comparison with coupled cluster calculations (see the Supporting Information). The model system reactants were built assuming a hydrogen bond between the pyrone hydroxyl group and the aniline nitrogen. In addition to a reference system for which R = H, both electron-donating (R = CH_3 or OCH_3) and electron-withdrawing substituents (R = CN or NO_2) were probed. On the basis of relaxed potential surface scans, all systems yielded a single transition state for the process in Figure 3B; the results are summarized in Table 1.

Table 1. Computed Free Energies of Activation (kilocalories per mole at 298 K) for the Reaction of Model System 14[a]

	$\Delta G^{\ddagger}$(298 K)	
reactant, R	ω-B97X-D	M06-2X
14a, H	24.3	26.5
14b, CH_3	24.0	25.7
14c, OCH_3	23.0	25.8
14d, CN	26.5	28.2
14e, NO_2	27.0	29.0

[a]Performed with PCM solvation (water) and using the 6-31+G(d,p) basis set.

Intrinsic reaction coordinate (IRC) calculations[32] were performed to assess the timing of different events. The representative IRC plot (for **14e**, R = NO_2) in Figure 3C shows, in addition to the relative energy, the distances for the formation of N···H bonds and the breaking of N···C bonds and suggests that the hydrogen is transferred from the O−H to the N well before the transition state, and the final portion of the barrier corresponds to breaking of the C−N bond. Thus, near the transition state the nitrogen has already become positively charged. The M06-2X-computed changes in charge, using CM5 charges,[33] are consistent with this idea (Table S42). The charge on the aniline nitrogen is predicted to change by +0.32 (becoming more positive) on going from **14a** to corresponding transition state **14a-TS**. The corresponding predicted changes in **14b**−**14e** are +0.31, +0.31, +0.34, and +0.34, respectively.

https://doi.org/10.1021/acs.joc.4c01377
J. Org. Chem. 2024, 89, 12432−12438

Consistent with the hypothesis that the transition state would be stabilized by electron-donating groups at the *para* position of the aniline and destabilized by electron-withdrawing groups, the computed free energy barrier at 298 K decreases for **14b** (R = CH_3) and **14c** (R = OCH_3), and it increases for **14d** (R = CN) and **14e** (R = NO_2), relative to the overall barrier of 24.3−26.5 kcal/mol computed for **14a** (Table 1). The same trends are predicted with both theoretical methods employed here.

Hydrolysis Experiment. In the absence of cysteine, hydrolysis of the **L1** and **L2** series was anticipated to generate hydroxy intermediate **9**, which would further degrade into aniline **7**, aldehyde **10**, and kojic acid (**11**). Close inspection of the resulting NMR spectra confirmed the absence of the C6 proton on kojic acid (consistent with the data presented by Jaudzems et al.),[12] prompting us to fully characterize the NMR spectrum of **L1A** after incubation for 3 h under hydrolysis conditions (Figure S5). In comparison to a 10 min time point, a growing signal was observed at 9.90 ppm, indicative of the aldehyde C−H of benzaldehyde (**10**). Similarly, the appearance of a second set of signals adjacent to the chemical shifts of the **L1A** leaving group enabled us to determine the presence of aniline (**7**). However, the appearance of signals in the range of 7.20−7.40 ppm could not be accounted for, and although a signal at 6.35 ppm was initially attributed to the C3 proton of kojic acid, the absence of an accompanying C6 proton at 7.90 ppm suggested the appearance of an uncharacterized byproduct.

Further insight was obtained through a series of NMR spiking experiments, in which compounds of interest were added to **L1A** after incubation for 3 h under hydrolysis conditions, and the resulting spectra were analyzed for the growth of existing signals versus the appearance of new ones (Figure 4). In comparison with the 10 min time point, the C3

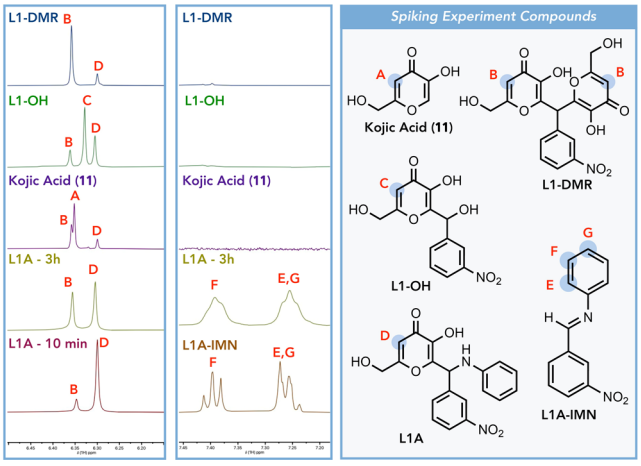

Figure 4. NMR spiking experiments in which suspected compounds of interest (right) were added to **L1A** after incubation for 3 h under hydrolysis assay conditions.

proton of **L1A** (labeled **D**) was observed to diminish, with the concomitant increase of a new singlet (**B**). Spiking with kojic acid (**11**) led to the appearance of a new signal (**A**), conclusively disproving the existence of **11** in the original spectrum. Surprisingly, upon spiking with a synthetic sample of hydroxy intermediate **L1-OH** (**9**), a new signal (**C**) was observed, suggesting that **9** was not formed under the reaction conditions either. In fact, **9** was observed to be completely stable under the assay conditions, with no appearance of **7**, **10**, or **11** after incubation for 3 h (Figure S6). These results strongly suggest that **9** is not a relevant intermediate in the hydrolysis pathway. We hypothesized that a retro-Mannich mechanism may instead be operative, consistent with the microscopic reversibility principle as applied to our forward synthetic strategy. If correct, we anticipated the formation of imine **L1-IMN**; indeed, spiking with a synthetic sample of **L1-IMN** resulted in the growth of two previously unidentified peaks in the range of 7.20−7.40 ppm, which could be assigned to positions **E**−**G** of **L1-IMN** (Figure 4, middle). However, a retro-Mannich mechanism would also be expected to deliver kojic acid (**11**), and its absence was previously noted.

To identify the origin of signal **B**, upscaling[34] of the hydrolysis assay was performed on **L1A**, and the resulting mixture was purified by preparative TLC (prep-TLC) (Figure S7). Characterization of the isolated prep-TLC bands confirmed the presence of all of the previously identified assay products [benzaldehyde (**10**), aniline (**7**), **L1A-IMN**, and unreacted **L1A**], in addition to one new product, **L1-DMR**, which incorporates two kojic acid residues. Having accounted for all of the NMR signals in the hydrolysis assay, we performed a final spiking experiment with a synthetic sample of **L1-DMR**, resulting in the growth of previously uncharacterized signal **B** (Figure 4, left).

Interestingly, **L1-DMR** was previously observed as a minor byproduct during the synthesis of the **L1** series.[35] The formation of **L1-DMR** was hypothesized to occur via conjugate addition of kojic acid (**11**) to Michael acceptor **8**, formed from the **L1** analogues via the aforementioned intramolecular proton transfer−retro-Michael sequence. Notably, the isolation of **L1-DMR** in the hydrolysis assay suggests that two distinct mechanistic pathways (the retro-Michael and retro-Mannich) are simultaneously operative and offer an explanation for the absence of **11** from the hydrolysis assay NMR spectra.

In the presence of a good nucleophile [such as cysteine (**15**)], the rate of inhibitor consumption is driven by the reversible formation of reactive Michael acceptor **8** (via retro-Michael), which is captured by an irreversible conjugate addition to form cysteine adduct **12** (Scheme 3). In the absence of a good nucleophile, the rate of inhibitor consumption is instead driven by the kinetically slower formation of kojic acid (**11**) via a retro-Mannich reaction,

Scheme 3. Mechanistic Proposal

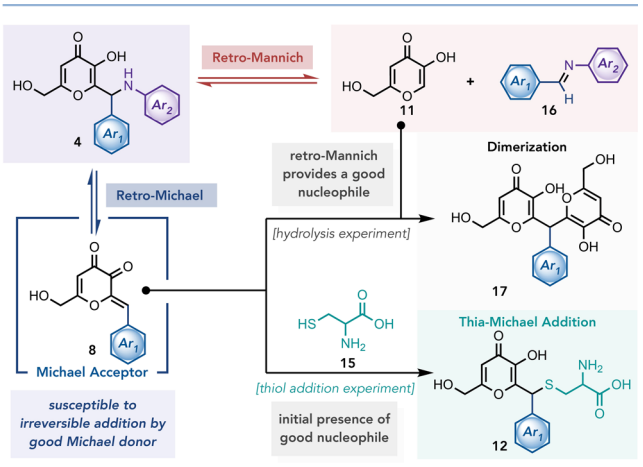

https://doi.org/10.1021/acs.joc.4c01377
J. Org. Chem. 2024, 89, 12432−12438

which serves as a nucleophilic trap for **8**, yielding dimerization adduct **17**. Notably, in the presence of cysteine, the formation of retro-Mannich products was not observed under the assay conditions.[36] Moreover, when kojic acid was added as an external nucleophile to the assay instead of cysteine, rapid formation of **17** was observed (at rates comparable to the rate of formation of the adduct **12**) (Figure S8).

Further evidence for this mechanistic proposal was obtained from Hammett analysis of the **L1** analogues under hydrolysis conditions (Figure 2B), which displayed a nonlinear correlation between substituent electronics and reaction rate. The proportionality constant was essentially flat for strongly donating and weakly withdrawing substituents ($\rho = -0.19$) but became significantly steeper for strongly withdrawing substituents ($\rho = -3.07$). Nonlinear correlations typically indicate a change in mechanism or rate-determining step (RDS).[37,38] For most substituents, a rate-determining retro-Mannich reaction appears to be operative, largely independent of LG electronics; for strongly withdrawing substituents, the retro-Michael reaction becomes significantly slower (vide supra) and likely becomes rate-determining. By contrast, the **L2** series displayed a linear and essentially flat proportionality constant ($\rho = -0.24$), suggesting that the electronics of the Ar_1 group do not play a significant role in transition state stability and are insufficient to trigger a change in RDS.

The purported rate-determining retro-Mannich reaction was further investigated through a solvent kinetic isotope effect (KIE) study using **L1A**, conducted by replacing D_2O with H_2O in the NMR buffer solution (Figure 5A). Surprisingly, the

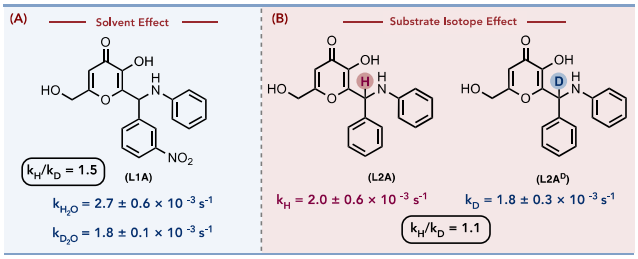

Figure 5. Kinetic isotope effect studies. (A) Solvent isotope effect values for hydrolysis were determined by subjecting **L1A** to either a D_2O-based assay buffer [k_{D_2O}; $(CD_3)_2SO$, 1× PBS buffer (prepared in D_2O), and D_2O in a 3.5:1.7:1 ratio, adjusted to pD 7.25 (pH 6.85)] or an H_2O-based assay buffer [k_{H_2O}; $(CD_3)_2SO$, 1× PBS buffer, and H_2O in a 3.5:1.7:1 ratio, adjusted to pH 7.25] at 25 °C. (B) Substrate isotope effect at the highlighted methine determined by subjecting **L2A** or **L2A^D** to an H_2O-based assay buffer.

k_H/k_D was found to be 1.5, a normal secondary KIE, suggesting that the transfer of readily exchangeable protons (aniline N−H, phenol O−H, or C6−H) was not itself rate-limiting.[39,40] A substrate KIE study was then conducted using **L2A^D**, with deuterium incorporated at the benzylic methine (90% D incorporation),[41] resulting in another normal secondary KIE ($k_H/k_D = 1.1$) (Figure 5B), consistent with an anticipated sp^3−sp^2 rehybridization[42,43] of the methine carbon during the retro-Mannich mechanism.

In summary, we have presented a thorough mechanistic analysis of a promising class of 5-hydroxy γ-pyrone Michael acceptor prodrugs, supporting the revision of a previously proposed mechanism. Our study elucidates the effect of substituent electronics on reaction rate and suggests that the mechanisms of inhibition and hydrolysis are distinct. The findings presented herein may inform the future design of optimized inhibitors against a variety of active site cysteines. Efforts to promote the cysteine addition pathway over hydrolysis using a prodrug strategy (i.e., converting substituents on Ar_2 from an EWG to an EDG with a biological stimulus) are currently ongoing in our laboratory.

■ ASSOCIATED CONTENT

Data Availability Statement

The data underlying this study are available in the published article and its Supporting Information.

Supporting Information

The Supporting Information is available free of charge at https://pubs.acs.org/doi/10.1021/acs.joc.4c01377.

General methods, synthetic procedures, experimental protocol for the quantitative kinetic NMR assay, data from NMR experiments, computational details, computed absolute energies and thermal corrections, optimized Cartesian coordinates, characterization data, and copies of ^{1}H NMR, ^{13}C NMR, ^{19}F NMR, COSY, HSQC, and HMBC spectra (PDF)

FAIR data, including the primary NMR FID files, for compounds **L1A**−**L1H**, **L1A-IMN**, **L1-DMR**, **L1-OH**, and **12** (ZIP)

FAIR data, including the primary NMR FID files, for compounds **L2A**−**L2H**, **L2A^D**, and **BA-d** (ZIP)

FAIR data, including the primary NMR FID files, for hydrolysis kinetic assays and kinetic isotope effect studies (ZIP)

FAIR data, including the primary NMR FID files, for cysteine kinetic assays (ZIP)

FAIR data, including the primary NMR FID files, for differential buffer kinetic assays (ZIP)

■ AUTHOR INFORMATION

Corresponding Author

Herman Nikolayevskiy − *Department of Chemistry, University of San Francisco, San Francisco, California 94117, United States*; orcid.org/0000-0002-4658-4182; Email: hnikolayevskiy@usfca.edu

Authors

Clifford Leung − *Department of Chemistry, University of San Francisco, San Francisco, California 94117, United States*

Umyeena M. Bashir − *Department of Chemistry, University of San Francisco, San Francisco, California 94117, United States*

William L. Karney − *Department of Chemistry, University of San Francisco, San Francisco, California 94117, United States*; orcid.org/0000-0003-0976-742X

Mark G. Swanson − *Department of Chemistry and Biochemistry, San Francisco State University, San Francisco, California 94132, United States*

Complete contact information is available at: https://pubs.acs.org/10.1021/acs.joc.4c01377

Author Contributions

H.N. and C.L. conceptualized the research study. M.G.S., C.L., and U.M.B. contributed to the design of the NMR kinetics assay. C.L. performed and analyzed all of the synthetic and kinetic experiments. C.L. and H.N. interpreted the mechanistic

https://doi.org/10.1021/acs.joc.4c01377
J. Org. Chem. 2024, 89, 12432−12438

data. W.L.K. conducted and analyzed all of the computational experiments. C.L., H.N., and W.L.K. prepared the manuscript and Supporting Information. All authors have given approval to the final version of the manuscript.

Notes

The authors declare no competing financial interest.

■ ACKNOWLEDGMENTS

This work was generously supported by the University of San Francisco Faculty Development Fund, the Whitehead Summer Research Fellowship, the Chemistry Department Summer Research Scholarship, and the National Science Foundation (W.L.K., CHE-2102160; M.G.S., DBI-1625721).

■ REFERENCES

(1) He, M.; Fan, M.; Peng, Z.; Wang, G. An Overview of Hydroxypyranone and Hydroxypyridinone as Privileged Scaffolds for Novel Drug Discovery. *Eur. J. Med. Chem.* **2021**, *221*, 113546−113574.

(2) Singh, S. B.; Zink, D. L.; Dombrowski, A. W.; Dezeny, G.; Bills, G. F.; Felix, J. P.; Slaughter, R. S.; Goetz, M. A. Candelalides A−C: Novel Diterpenoid Pyrones from Fermentations of *Sesquicillium candelabrum* as Blockers of the Voltage-Gated Potassium Channel Kv1.3. *Org. Lett.* **2001**, *3* (2), 247−250.

(3) Kurosawa, K.; Takahashi, K.; Tsuda, E. SNF4435C and D, Novel Immunosuppressants Produced by a Strain of Streptomyces Spectabilis. I. Taxonomy, Fermentation, Isolation and Biological Activities. *J. Antibiot. (Tokyo)* **2001**, *54* (7), 541−547.

(4) Ui, H.; Shiomi, K.; Suzuki, H.; Hatano, H.; Morimoto, H.; Yamaguchi, Y.; Masuma, R.; Sunazuka, T.; Shimamura, H.; Sakamoto, K.; Kita, K.; Miyoshi, H.; Tomoda, H.; Ōmura, S. Verticipyrone, a New NADH-Fumarate Reductase Inhibitor, Produced by Verticillium Sp. FKI-1083. *J. Antibiot.* **2006**, *59*, 785−790.

(5) Watanabe, K.; Iwasaki, K.; Abe, T.; Inoue, M.; Ohkubo, K.; Suzuki, T.; Katoh, T. Enantioselective Total Synthesis of (−)-Candelalide A, a Novel Blocker of the Voltage-Gated Potassium Channel Kv1.3 for an Immunosuppressive Agent. *Org. Lett.* **2005**, *7* (17), 3745−3748.

(6) Parker, K. A.; Lim, Y.-H. The Total Synthesis of (−)-SNF4435 C and (+)-SNF4435 D. *J. Am. Chem. Soc.* **2004**, *126* (49), 15968−15969.

(7) Shimamura, H.; Sunazuka, T.; Izuhara, T.; Hirose, T.; Shiomi, K.; Ōmura, S. Total Synthesis and Biological Evaluation of Verticipyrone and Analogues. *Org. Lett.* **2007**, *9* (1), 65−67.

(8) Zhang, Z.; Tang, W. Drug Metabolism in Drug Discovery and Development. *Acta Pharm. Sin. B* **2018**, *8* (5), 721−732.

(9) Wen, A.; Qin, A. R.-R.; Tarnowski, T.; Ling, K. H. J.; Zhang, H.; Humeniuk, R.; Regan, S.; Saquing, J.; Liu, W.; Venkatarangan, L.; Xiao, D. Plasma Protein Binding Determination for Unstable Ester Prodrugs: Remdesivir and Tenofovir Alafenamide. *J. Pharm. Sci.* **2023**, *112* (12), 3224−3232.

(10) Buettner, R.; Corzano, R.; Rashid, R.; Lin, J.; Senthil, M.; Hedvat, M.; Schroeder, A.; Mao, A.; Herrmann, A.; Yim, J.; Li, H.; Yuan, Y.-C.; Yakushijin, K.; Yakushijin, F.; Vaidehi, N.; Moore, R.; Gugiu, G.; Lee, T. D.; Yip, R.; Chen, Y.; Jove, R.; Horne, D.; Williams, J. C. Alkylation of Cysteine 468 in Stat3 Defines a Novel Site for Therapeutic Development. *ACS Chem. Biol.* **2011**, *6* (5), 432−443.

(11) A detailed exploration of buffer identity and NaCl content suggests that ionic strength plays an important role in the differential hydrolytic stability observed by: Karatas, H.; Akbarzadeh, M.; Adihou, H.; Hahne, G.; Pobbati, A. V.; Yihui Ng, E.; Guéret, S. M.; Sievers, S.; Pahl, A.; Metz, M.; Zinken, S.; Dötsch, L.; Nowak, C.; Thavam, S.; Friese, A.; Kang, C.; Hong, W.; Waldmann, H. Discovery of Covalent Inhibitors Targeting the Transcriptional Enhanced Associate Domain Central Pocket. *J. Med. Chem.* **2020**, *63* (20), 11972−11989. (see Section 4.4 of the Supporting Information).

(12) Jaudzems, K.; Kurbatska, V.; Jēkabsons, A.; Bobrovs, R.; Rudevica, Z.; Leonchiks, A. Targeting Bacterial Sortase A with Covalent Inhibitors: 27 New Starting Points for Structure-Based Hit-to-Lead Optimization. *ACS Infect. Dis.* **2020**, *6* (2), 186−194.

(13) Cascioferro, S.; Raffa, D.; Maggio, B.; Raimondi, M. V.; Schillaci, D.; Daidone, G. Sortase A Inhibitors: Recent Advances and Future Perspectives. *J. Med. Chem.* **2015**, *58* (23), 9108−9123.

(14) Maresso, A. W.; Wu, R.; Kern, J. W.; Zhang, R.; Janik, D.; Missiakas, D. M.; Duban, M.-E.; Joachimiak, A.; Schneewind, O. Activation of Inhibitors by Sortase Triggers Irreversible Modification of the Active Site. *J. Biol. Chem.* **2007**, *282* (32), 23129−23139.

(15) Greenwald, R. B.; Pendri, A.; Conover, C. D.; Zhao, H.; Choe, Y. H.; Martinez, A.; Shum, K.; Guan, S. Drug Delivery Systems Employing 1,4- or 1,6-Elimination: Poly(Ethylene Glycol) Prodrugs of Amine-Containing Compounds. *J. Med. Chem.* **1999**, *42* (18), 3657−3667.

(16) Gavriel, A. G.; Sambrook, M. R.; Russell, A. T.; Hayes, W. Recent Advances in Self-Immolative Linkers and Their Applications in Polymeric Reporting Systems. *Polym. Chem.* **2022**, *13* (22), 3188−3269.

(17) The Merck Index Online - chemicals, drugs and biologicals. https://merckindex.rsc.org/ (accessed 2024-04-03).

(18) Wang, Y.; Fan, H.; Balakrishnan, K.; Lin, Z.; Cao, S.; Chen, W.; Fan, Y.; Guthrie, Q. A.; Sun, H.; Teske, K. A.; Gandhi, V.; Arnold, L. A.; Peng, X. Hydrogen Peroxide Activated Quinone Methide Precursors with Enhanced DNA Cross-Linking Capability and Cytotoxicity towards Cancer Cells. *Eur. J. Med. Chem.* **2017**, *133*, 197−207.

(19) Leung, C.; Bashir, U. M.; Karney, W. L.; Swanson, M. G.; Nikolayevskiy, H. Mechanistic Analysis of 5-Hydroxy γ-Pyrones as Michael Acceptor Prodrugs. *ChemRxiv* **2024**, DOI: 10.26434/chemrxiv-2024-nbc5g-v2.

(20) 3-Nitrobenzaldehyde was selected through a series of screening reactions of various benzaldehyde derivatives to initially observe the highest conversion of the coupled product.

(21) Phillips, J.; Barrall, E. Betti Reactions of Some Phenols. *J. Org. Chem.* **1956**, *21* (6), 692−694.

(22) O'Brien, G.; Patterson, J. M.; Meadow, J. R. Amino Derivatives of Kojic Acid. *J. Org. Chem.* **1960**, *25* (1), 86−89.

(23) Guzen, K. P.; Guarezemini, A. S.; Órfão, A. T. G.; Cella, R.; Pereira, C. M. P.; Stefani, H. A. Eco-Friendly Synthesis of Imines by Ultrasound Irradiation. *Tetrahedron Lett.* **2007**, *48* (10), 1845−1848.

(24) Glasoe, P. K.; Long, F. A. Use of Glass Electrodes to Measure Acidities in Deuterium Oxide. *J. Phys. Chem.* **1960**, *64* (1), 188−190.

(25) (a) Hammett, L. P. The Effect of Structure upon the Reactions of Organic Compounds. Benzene Derivatives. *J. Am. Chem. Soc.* **1937**, *59* (1), 96−103. (b) Hansch, C.; Leo, A.; Taft, R. W. A Survey of Hammett Substituent Constants and Resonance and Field Parameters. *Chem. Rev.* **1991**, *91* (2), 165−195.

(26) Characterization data for cysteine adduct **12** (Ar_1 = *m*-NO_2) are presented in the Supporting Information.

(27) Two possibilities were considered. (a) The aniline LG leaves with a negative charge. (b) The initial protonation of the aniline nitrogen leads to a zwitterionic intermediate that would result in a loss of positive charge during C···N bond scission.

(28) Chai, J.-D.; Head-Gordon, M. Long-Range Corrected Hybrid Density Functionals with Damped Atom−Atom Dispersion Corrections. *Phys. Chem. Chem. Phys.* **2008**, *10* (44), 6615−6620.

(29) Zhao, Y.; Truhlar, D. G. The M06 Suite of Density Functionals for Main Group Thermochemistry, Thermochemical Kinetics, Noncovalent Interactions, Excited States, and Transition Elements: Two New Functionals and Systematic Testing of Four M06-Class Functionals and 12 Other Functionals. *Theor. Chem. Acc.* **2008**, *120* (1−3), 215−241.

(30) Cossi, M.; Barone, V.; Cammi, R.; Tomasi, J. Ab Initio Study of Solvated Molecules: A New Implementation of the Polarizable Continuum Model. *Chem. Phys. Lett.* **1996**, *255* (4−6), 327−335.

(31) All calculations were performed with *Gaussian 16*: Frisch, M. J.; Trucks, G. W.; Schlegel, H. B.; Scuseria, G. E.; Robb, M. A.;

Cheeseman, J. R.; Scalmani, G.; Barone, V.; Petersson, G. A.; Nakatsuji, H.; Li, X.; Caricato, M.; Marenich, A. V.; Bloino, J.; Janesko, B. G.; Gomperts, R.; Mennucci, B.; Hratchian, H. P.; Ortiz, J. V.; Izmaylov, A. F.; Sonnenberg, J. L.; Williams-Young, D.; Ding, F.; Lipparini, F.; Egidi, F.; Goings, J.; Peng, B.; Petrone, A.; Henderson, T.; Ranasinghe, D.; Zakrzewski, V. G.; Gao, J.; Rega, N.; Zheng, G.; Liang, W.; Hada, M.; Ehara, M.; Toyota, K.; Fukuda, R.; Hasegawa, J.; Ishida, M.; Nakajima, T.; Honda, Y.; Kitao, O.; Nakai, H.; Vreven, T.; Throssell, K.; Montgomery, J. A., Jr.; Peralta, J. E.; Ogliaro, F.; Bearpark, M. J.; Heyd, J. J.; Brothers, E. N.; Kudin, K. N.; Staroverov, V. N.; Keith, T. A.; Kobayashi, R.; Normand, J.; Raghavachari, K.; Rendell, A. P.; Burant, J. C.; Iyengar, S. S.; Tomasi, J.; Cossi, M.; Millam, J. M.; Klene, M.; Adamo, C.; Cammi, R.; Ochterski, J. W.; Martin, R. L.; Morokuma, K.; Farkas, O.; Foresman, J. B.; Fox, D. J. *Gaussian 16*, rev. C.01; Gaussian, Inc., Wallingford, CT, 2019.

(32) (a) Fukui, K. A Formulation of the Reaction Coordinate. *J. Phys. Chem.* **1970**, *74* (23), 4161−4163. (b) Fukui, K. The Path of Chemical Reactions − The IRC Approach. *Acc. Chem. Res.* **1981**, *14* (12), 363−368. (c) Hratchian, H. P.; Schlegel, H. B. Finding Minima, Transition States, and Following Reaction Pathways on *Ab Initio* Potential Energy Surfaces. In *Theory and Applications of Computational Chemistry: The First Forty Years*; Dykstra, C. E., Frenking, G., Kim, K. S., Scuseria, G., Eds.; Elsevier: Amsterdam, 2005; pp 195−249.

(33) Marenich, A. V.; Jerome, S. V.; Cramer, C. J.; Truhlar, D. G. Charge Model 5: An Extension of Hirshfeld Population Analysis for the Accurate Description of Molecular Interactions in Gaseous and Condensed Phases. *J. Chem. Theory Comput.* **2012**, *8* (2), 527−541.

(34) A 20-fold upscaling of the assay under hydrolysis conditions was performed for **L1A** to provide enough compound for isolation and characterization.

(35) The dimer product was also observed during the synthesis of the **L2** analogue series.

(36) Bolton, J. L.; Turnipseed, S. B.; Thompson, J. A. Influence of Quinone Methide Reactivity on the Alkylation of Thiol and Amino Groups in Proteins: Studies Utilizing Amino Acid and Peptide Models. *Chem. Biol. Interact.* **1997**, *107* (3), 185−200.

(37) Schreck, J. O. Nonlinear Hammett Relationships. *J. Chem. Educ.* **1971**, *48* (2), 103−107.

(38) Willi, A. V.; Robertson, R. E. A Kinetic Study Of the Hydrolysis of Benzalaniline. *Can. J. Chem.* **1953**, *31* (4), 361−376.

(39) Westheimer, F. H. The Magnitude of the Primary Kinetic Isotope Effect for Compounds of Hydrogen and Deuterium. *Chem. Rev.* **1961**, *61* (3), 265−273.

(40) Nesheim, J. C.; Lipscomb, J. D. Large Kinetic Isotope Effects in Methane Oxidation Catalyzed by Methane Monooxygenase: Evidence for C−H Bond Cleavage in a Reaction Cycle Intermediate. *Biochemistry* **1996**, *35* (31), 10240−10247.

(41) Li, X.; Wu, S.; Chen, S.; Lai, Z.; Luo, H.-B.; Sheng, C. One-Pot Synthesis of Deuterated Aldehydes from Arylmethyl Halides. *Org. Lett.* **2018**, *20* (7), 1712−1715.

(42) Streitwieser, A.; Jagow, R. H.; Fahey, R. C.; Suzuki, S. Kinetic Isotope Effects in the Acetolyses of Deuterated Cyclopentyl Tosylates. *J. Am. Chem. Soc.* **1958**, *80* (9), 2326−2332.

(43) Gómez-Gallego, M.; Sierra, M. A. Kinetic Isotope Effects in the Study of Organometallic Reaction Mechanisms. *Chem. Rev.* **2011**, *111* (8), 4857−4963.

https://doi.org/10.1021/acs.joc.4c01377
J. Org. Chem. 2024, 89, 12432−12438